Artery Research (2018) 23, 56–62

Available online at www.sciencedirect.com

ScienceDirect

journal homepage: www.elsevier.com/locate/artres

Modeling radial artery pressure waveforms using curve fitting: Comparison of four types of fitting functions

Xinge Jiang [a,b], Shoushui Wei [a,*], Jingbo Ji [b], Feifei Liu [c], Peng Li [a], Chengyu Liu [c,**]

[a] School of Control Science and Engineering, Shandong University, Jinan, 250061, China
[b] Shandong College of Electronic Technology, Jinan, 250200, China
[c] The State Key Laboratory of Bioelectronics, Jiangsu Key Lab of Remote Measurement and Control, School of Instrument Science and Engineering, Southeast University, Nanjing, 210096, China

Received 15 July 2018; received in revised form 1 August 2018; accepted 20 August 2018

KEYWORDS
Curve fitting;
Raleigh function;
Double-exponential function;
Gaussian function;
Logarithmic normal function;
Radial artery pressure waveform (RAPW);
Mean absolute error

Abstract *Background:* Curve fitting has been intensively used to model artery pressure waveform (APW). The modelling accuracy can greatly influence the calculation of APWs parameters that serve as quantitative measures for assessing the morphological characteristics of APWs. However, it is unclear which fitting function is more suitable for APW. In this paper, we compared the fitting accuracies of four types of fitting functions, including Raleigh function, double-exponential function, Gaussian function, and logarithmic normal function, in modeling radial artery pressure waveform (RAPW).
Methods: RAPWs were recorded from 24 healthy subjects in resting supine position. To perform curve fitting, 10 consecutive stable RAPWs for each subject were randomly selected and each waveform was fitted using three instances of the same fitting function.
Results: The mean absolute percentage errors (MAPE) of the fitting results were 5.89% ± 0.46% (standard deviation), 3.31% ± 0.22%, 2.25% ± 0.31%, and 1.49% ± 0.28% for Raleigh function, double-exponential function, Gaussian function, and logarithmic normal function, respectively. Their corresponding mean maximum residual errors were 23.71%, 17.83%, 6.11%, and 5.49%.
Conclusions: The performance of using Gaussian function and logarithmic normal function to model RAPW is comparable, and is better than that of using Raleigh function and double-exponential function.

* Corresponding author.
** Corresponding author.
E-mail addresses: sswei@sdu.edu.cn (S. Wei), chengyu@seu.edu.cn (C. Liu).

https://doi.org/10.1016/j.artres.2018.08.003

Introduction

It has been widely accepted that changes of artery pressure waveform (APW) characteristics are risk indicators of cardiovascular diseases.[1–3] Pulse transit time (PTT), pulse wave velocity (PWV), and reflection index (RI) have been derived from APWs as parameters of clinical interest.[1,4–6] Many techniques are used to obtain information on human physiology or pathology by studying changes in APWs. Traditionally, derivative methods can acquire the morphological changes of APWs by extracting parameters and wave intensity analysis can obtain changes of wave reflections in the nature and timing according to APWs' pressure and flow velocity.[7–10] Though simple and can be used for real-time computing are the advantages of these technologies, they fail to analyze the features of the complete APWs and their performance is relatively poor when APWs are weak and noisy.

Curve fitting has been intensively studied recently to quantitatively assess the morphological changes of APWs. APW is a composite of a forward wave and a reflected wave.[11] Each wave can be approximated by a fitting function. The change of APW is completely reflected by the parameter changes of the fitting function. Whether or not the reflected wave can be found in an intuitive way, this analysis method can easily represent the reflected wave and make the characteristics of APW very clear. The fitting parameters are obtained by least squares method, which is a macroscopic method, so it can effectively suppress noise and greatly improve the precision of measurement. Several different fitting functions have been applied, e.g., triangular function,[12] Raleigh function,[13] Gaussian function,[14] and logarithmic normal function.[15] Among them, triangular function showed much deviation between the fitting result and original waveform and is thus rarely used currently.[12] A mean square error (MSE) of $<0.5\%$ was achieved in reconstructing finger photoplethysmographic (PPG) waveform using two Raleigh functions.[13] An average maximum residue error of 4% was reported based on five logarithmic normal function to decompose finger and tip PPG waveform.[15,16] Four Gaussian functions resulted in a residual error of $<10\%$ for decomposing ear and finger PPG.[14] To reconstruct the digital volume pulse waveform detected on the left index finger, four or five Gaussian functions were used with both suggesting a root mean square error of $<2.0\%$.[17] A similar fitting approach using five Gaussian functions has also been applied in order for extracting feature points from finger PPG.[18] For modelling carotid and radial APWs, Liu et al. have demonstrated that three positive Gaussian functions are already optimal, resulting in a mean absolute percentage error (MAPE) of as low as 1.1% and 1.0%, respectively, for carotid and radial APWs.[19] Double-exponential often has been used as fitting functions for corona discharge and high voltage[20] and bimodal waveform occasionally appears in sleep apnea patients' waveforms obtained from finger PPG, which is what we will study next. In this paper double-exponential has been used as contrast fitting function.

The modelling accuracy can greatly influence the calculation of APWs parameters that serve as quantitative measures for assessing the morphological characteristics of APWs. However, it is unclear which fitting function is more appropriate, even though relatively low fitting errors have been reported for all those functions. Besides, APWs detected at different sites have been used in those studies which makes the results less comparable. In this work, we aimed to compare the performance of four fitting functions, i.e., Raleigh function, logarithmic normal function, Gaussian function, and double-exponential function to model the APWs collected at the radial site.

Methods

Data

Data used in this paper came from our previous study.[21] Table 1 shows the participants' basic clinical information. Ethical permission was received from the ethical committee of Shandong Provincial Hospital and all participants gave their informed consent. In short, the radial artery pressure waveform (RAPW) of right arm were recorded for 40 s with a sampling rate of 500 Hz by piezoelectric sensor from 24 healthy participants in a supine position and then were filtered by the band-pass filter (0.05—35 Hz). An open-source algorithm[22,23] was used to detect the feet of each recording and 10 successive normal sinus cardiac cycles were intercepted based on the feet, then 10 separate beats were extracted respectively between two adjacent pulse feet. Each separate beat was normalized to eliminate pressure effects, that was, each separate beat was finally to having a fixed length of 1000 (by interpolation) and 1-unit amplitude (i.e., pulse foot has an amplitude of 0 and pulse peak of 1).

Reconstruction of RAPW using curve fitting

Curve fitting was performed to reconstruct each specific RAPW segment. Here, we examined four different fitting functions:

i) *Raleigh function as defined by*:

$$f_k(n) = A_k \times n \times \exp\left(-\frac{1}{2} \times W_k \times n^2\right) \quad (1)$$

wherein $n = 1, 2, \ldots, 1000$ (i.e., the length of Raleigh function is 1000 points). The subscript k represents

Table 1 The 24 participants' basic clinical information.

Variables	Value	Range (min—max)
Number (M/F)	24 (14/10)	—
Age (year)	29 ± 8	21—50
Height	169 ± 8	151—183
Weight (kg)	63 ± 11	41—87
BMI (kg/m^2)	22 ± 3	15—27
SBP (mmHg)	115 ± 12	93—137
DBP (mmHg)	70 ± 10	57—95
MAP (mmHg)	85 ± 10	69—107

Value: mean ± SD.

different Raleigh functions with $k = 1, 2, 3$ and defined by the two parameters: A_k ($0 < A_k < 1000$) and W_k ($0 < W_k < 2000$).

ii) *Double-exponential function as defined by*:

$$f_k(n) = A_k \times \frac{1}{2b_k} \times \exp\left(-\frac{|n - a_k|}{b_k}\right) \quad (2)$$

wherein $n = 1, 2, \ldots, 1000$ that determines the length of the function and the subscript k represents different functions with $k = 1, 2, 3$ and determined by the three parameters: A_k ($0 < A_k < 1000$), a_k ($0 < a_k < 1000$), and ($0 < b_k < 1000$).

iii) *Gaussian function which is defined by*:

$$f_k(n) = H_k \times \exp\left(-\frac{2(n - C_k)^2}{W_k^2}\right) \quad (3)$$

Similarly, $n = 1, 2, \ldots, 1000$ and k indicates different Gaussian functions with $k = 1, 2, 3$ and determined by three parameters: H_k ($0 < H_k < 1$), W_k ($0 < W_k < 1000$), and C_k ($1 < C_1 < C_2 < C_3$).

iv) *Logarithmic normal function which is defined by*:

$$f_k(n) = \frac{1000 \times A_k}{\sqrt{2\pi} \times W_k \times n} \exp\left(-\frac{\left(\ln\left(\frac{n}{1000 \times X_{ck}}\right)\right)^2}{2W_k^2}\right) \quad (4)$$

Still, $n = 1, 2, \ldots, 1000$ and k represents different Logarithmic normal functions with $k = 1, 2, 3$ and defined by three parameters: A_k ($0 < A_k < 1$), W_k ($0 < W_k < 1$), and X_{ck} ($0 < X_{ck} < 1$).

Liu et al. have reported that using three positive Gaussian functions can accurately and reliably model radial pulses.[19] For each of the four fitting function types (Raleigh function, double-exponential function, Gaussian function and logarithmic normal function), three sub-functions are superimposed, i.e., $F(n) = \sum_{k=1}^{3} f_k(n)$, for fitting the original normalized pulse. Two-Stage particle swarm optimizer (TSPSO) was used in this work to determine the optimal parameters for the three functions. The suitability of TSPSO algorithm and its superiority compared to other optimization algorithms such as Nelder-Mead and modified particle swarm optimization (MPSO) have been confirmed in a previous study.[24] The normalized measurement signal was represented by S(n) and the fitting result function was represented by F(n). The optimization was targeting at

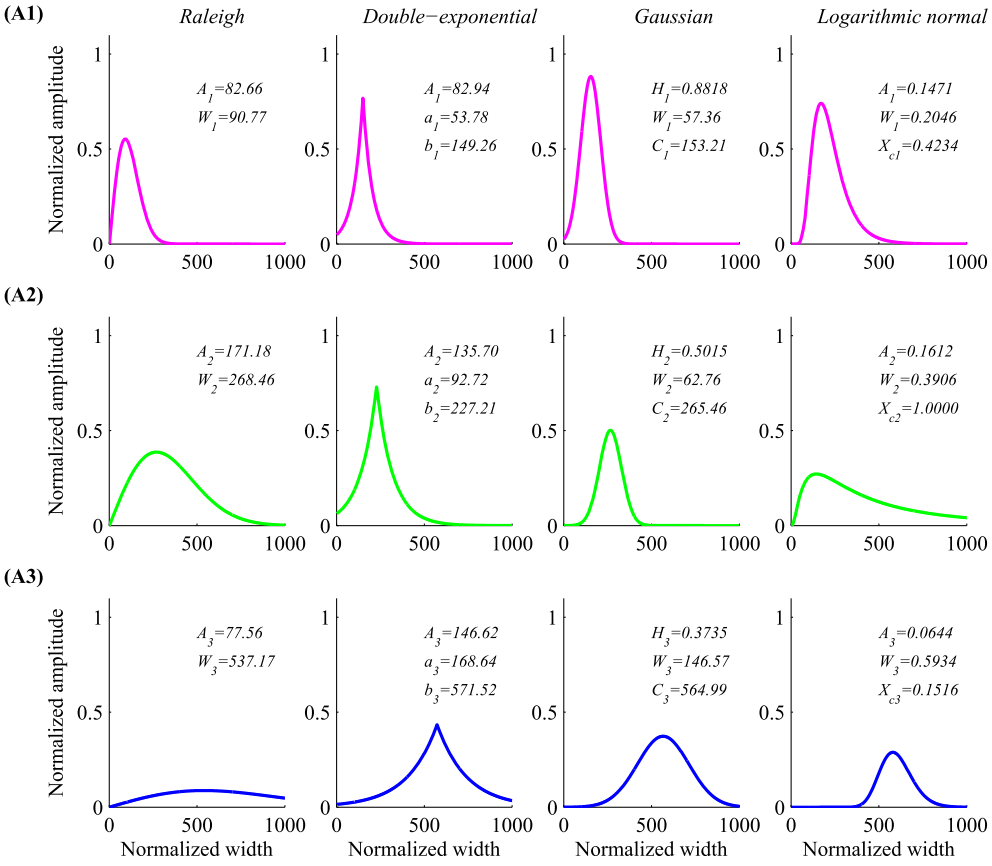

Figure 1 An example of three realizations (top to bottom panels) of the four fitting functions (left to right panels: Raleigh, double-exponential, Gaussian and logarithmic normal) with different combination of parameters.

minimization of the mean absolute percentage error (MAPE):

$$MAPE = \frac{\sum_{n=1}^{N} |F(n) - S(n)|}{N} \times 100\% \quad (5)$$

and the max residual (Max_R):

$$Max\_R = \max(|F(n) - S(n)|) \quad (n = 1, 2, \cdots, N) \quad (6)$$

two indices that were used in this study as criteria to determine the fitting accuracy.

Figure 1 illustrates separately three realizations of the four fitting functions with different combinations of parameters obtained by TSPSO for reconstructing a normalized RAPW segment.

Statistical analysis

For each subject, the mean MAPE and Max_R were calculated by averaging the results of 10 RAPWs segments. The overall mean and standard deviation[11] of MAPE and Max_R were then obtained across the 24 subjects. Performance of the four fitting functions in term of MAPE and Max_R were compared using paired T test. Analysis of paired T test was performed to investigate the difference of MAPE/Max_R error between four functions comparing each other. Statistical significance is considered if $P < 0.05$.

Results

Example of fitting results for a same RAPW segment using the four fitting functions are summarized in Fig. 2. Figure 2

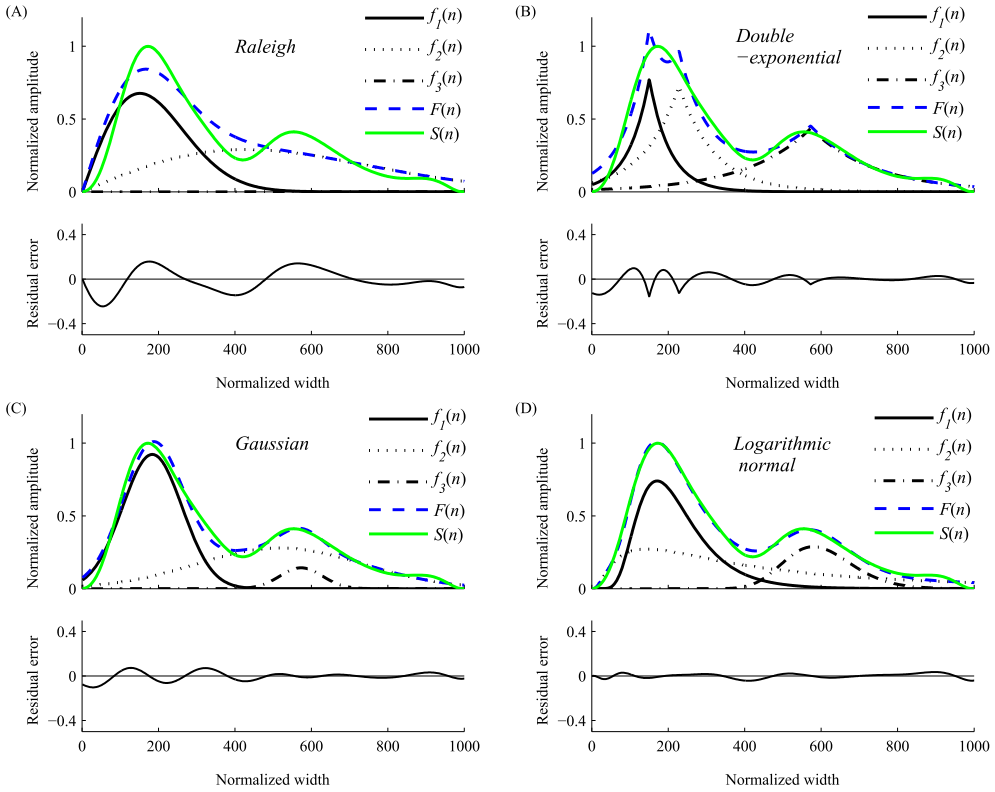

Figure 2 An example of waveform fitting using four fitting functions. (A) Raleigh function, (B) Double-exponential function, (C) Gaussian function, and (D) Logarithmic normal function. $S(n)$: the original normalized pulse; $F(n)$: the fitting result function; $f_1(n)$, $f_2(n)$ and $f_3(n)$: three sub-fitting functions. In the bottom of each subfigure, the residual error of fitting function was showed.

Table 2 Four fitting function's overall means and SDs of MAPE and Max_R values from 24 subjects.

Function	MAPE (%)		Max_R (%)	
	Mean	SD	Mean	SD
Raleigh	5.89 (4.71–8.35)	0.46 (0.22–0.90)	23.71 (21.38–25.77)	0.56 (0.32–1.13)
Double-exponential	3.31 (2.83–3.82)	0.22 (0.06–0.54)	17.83 (14.62–20.72)	1.06 (0.18–3.25)
Gaussian	2.25 (1.35–3.24)	0.31 (0.13–0.67)	6.11 (3.59–8.82)	0.99 (0.19–2.13)
Logarithmic normal	1.49 (0.88–2.27)	0.28 (0.07–0.78)	5.49 (3.10–7.51)	0.54 (0.26–2.19)

Note: Values were expressed as mean (minimum, maximum).

shows the accuracy of curve fitting using different fitting functions in term of residual error for each individual.

Table 2 show the performance of the four fitting functions for all 24 subjects. There are essentially different for MAPE between four functions comparing each other (all $P < 0.01$). Raleigh function has the biggest MAPE, while logarithmic normal function has the smallest MAPE. As for Max_R, Raleigh function and double-exponential function have larger compared to the other two (all $P < 0.01$). Logarithmic normal function and Gaussian function have comparable performance with $P > 0.18$.

Discussion

In this study, we compared the fitting accuracies of four fitting functions, i.e., Raleigh function, double-exponential function, Gaussian function, and logarithmic normal function, for reconstructing RAPWs. Overall, Gaussian function and logarithmic normal function showed comparable performance in term of MAPE (2.25% and 1.49%, respectively) and Max_R (6.11% and 5.49%, respectively), whereas Raleigh function and double-exponential function displayed worse performance (MAPE: 5.89% and 3.31%; Max_R: 23.71% and 17.83%).

The accuracy of fitting function can greatly influence the calculation of APWs parameters that serve as quantitative measures for assessing the morphological characteristics of APWs. It should note that pulse curve fitting is only the first step for clinical pulse analysis. By decomposing the pulse waveforms into different types of sub-waveform components, especially into the forward and backward sub-waveform components, we can obtain the clinically relevant features, and thus to help the doctors for the further disease diagnosis. For these application, typical examples existed: such as logarithmic normal function-based analysis for the estimation and determination of arterial elasticity,[15] Gaussian functions-based analysis for cardiovascular diseases diagnosis.[25] We identify this point as our future work, to explore the relationship between sub-waveform features and clinical diseases.

At different collecting locations, the peripheral APWs show different contours or shapes.[26] It is possible that the accuracies of fitting functions vary across different waveform contours. As a first step to explore this hypothesis, Fig. 3 and Table 3 show the accuracies of four fitting functions for modeling three APW segments that have different contours. For waveforms showed from Fig. 3 (A1) to (A3), the accuracies of Raleigh, Gaussian and logarithmic normal become worse with bigger MAPE, while the accuracy

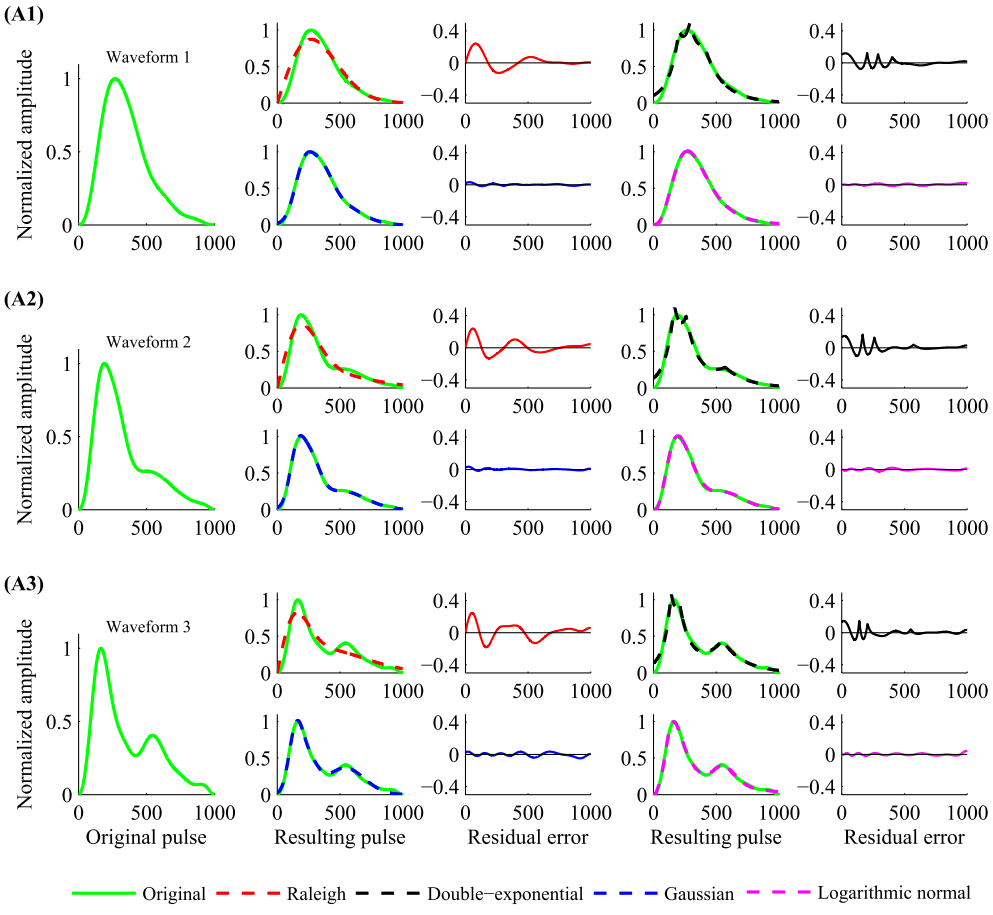

Figure 3 Three APWs with different contours were reconstructed by four fitting functions. On the left side of (A1), (A2) and (A3), the original waveforms are shown. The middle and right panels of (A1), (A2) and (A3) show the fitting results superimposed on the original waveform with the residual error plotted next to the fitting results.

Table 3 The accuracy of four fitting functions by decomposing three APWs with different contours.

Original pulse	Raleigh		Double-exponential		Gaussian		Logarithmic normal	
	MAPE (%)	Max_R (%)	MAPE (%)	Max_R (%)	MAPE (%)	Max_R (%)	MAPE (%)	Max_R (%)
Waveform 1	5.88	24.08	3.10	12.36	0.66	3.54	0.85	2.21
Waveform 2	6.01	23.86	3.03	16.47	0.74	3.38	0.87	2.47
Waveform 3	7.39	24.53	2.72	14.65	1.87	4.94	0.99	4.23

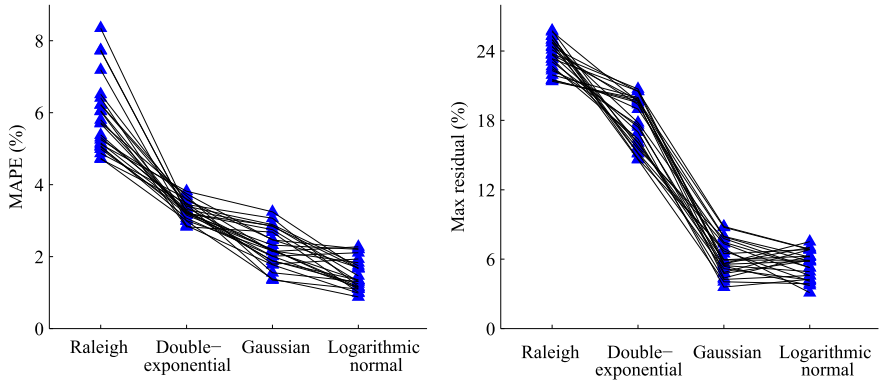

Figure 4 Individual results of the means MAPE and Max_R of the 24 subjects.

of double-exponential becomes better with smaller MAPE. For cases shown in Fig. 3 (A1) and (A2), Gaussian function shows the best performance with the smallest MAPE of 0.66% and 0.74%, respectively. For Fig. 3 (A2), logarithmic normal function shows the best performance with the smallest MAPE of 0.99%. Previously published studies may have concluded differently regarding which fitting function performs best. These preliminary results reported here demonstrate that it is possible that different sites for collecting data that have been applied in previous studied lead to the discrepancies.

Even though a same collecting site is used, the contours may vary dramatically because of individual difference, different operators, and different sensors, etc. Figure 4 shows the individual results of the means MAPE and Max_R of 24 subjects using the four functions. The result showed there are some differences for different people's MAPE and Max_R obtained by the same type of function. It is understandable that there are some differences of the accuracy of Gaussian function between our results and Liu's (MAPE: 2.25% and 1.1%, respectively) for APWs acquired from radial.[19,24]

One of the limitations of the current study is the relatively small sample size. However, within-subject comparison has been applied to examine the performance across different fitting functions which improves our statistical power. Besides, all participants in this study are healthy without known cardiovascular concerns. Future studies are warranted to further investigate whether the fitting model still works for patients with different cardiovascular diseases. We also note that three realizations of each fitting functions have been applied. This was based on a previous study that used Gaussian functions to model the RAPW and examined the performance of different amounts of realizations.[19]

In conclusion, we compared the accuracy of four fitting functions, i.e., Raleigh function, double-exponential function, Gaussian function, and logarithmic normal function, to model a same RAPWs data sets. Our results suggest that for modelling RAPWs, Gaussian function and logarithmic normal function could result in better accuracies compared to Raleigh function and double-exponential function.

Conflict of interest statement

The authors declare no conflict of interest.

Acknowledgements

This work was supported by the National Natural Science Foundation of China under grants 61671275 and 61201049, and Shandong Province Key Research and Development Plan under Grant 2018GSF118133.

References

1. Cohn JN, Finkelstein S, Mcveigh G, Morgan D, Lemay L, Robinson J, et al. Noninvasive pulse wave analysis for the early detection of vascular disease. *Hypertension* 1995;**26**(3):503—8.
2. Arnett DK, Boland LL, Evans GW, Riley W, Barnes R, Tyroler HA, et al. Hypertension and arterial stiffness: the atherosclerosis risk in communities study. *Am J Hypertens* 2000;**13**(4):317—23.
3. Sheen YJ, Lin JL, Li TC, Bau CT, Sheu WH. Peripheral arterial stiffness is independently associated with a rapid decline in estimated glomerular filtration rate in patients with type 2 diabetes. *BioMed Res Int* 2013;**2013**:309294.
4. Zheng D, Murray A. Peripheral arterial volume distensibility: significant differences with age and blood pressure measured using an applied external pressure. *Physiol Meas* 2011;**32**(5):499—512.

5. Avolio A. The finger volume pulse and assessment of arterial properties. *J Hypertens* 2002;**20**(12):2341—3.
6. Pucci G, Battista F, Anastasio F, Sanesi L, Gavish B, Butlin M, et al. Effects of gravity-induced upper-limb blood pressure changes on wave transmission and arterial radial waveform. *J Hypertens* 2016;**34**(6):1091.
7. Millasseau SC, Kelly RP, Ritter JM, Chowienczyk PJ. Determination of age-related increases in large artery stiffness by digital pulse contour analysis. *Clin Sci* 2002;**103**(4):371—7.
8. Bortolotto LA, Blacher J, Kondo T, Takazawa K, Safar ME. Assessment of vascular aging and atherosclerosis in hypertensive subjects: second derivative of photoplethysmogram versus pulse wave velocity. *Am J Hypertens* 2000;**13**(2):165—71.
9. Karamanoglu M. A system for analysis of arterial blood pressure waveforms in humans. *Comput Biomed Res Int J* 1997;**30**(3):244—55.
10. Zambanini A, Cunningham SL, Parker KH, Khir AW, McG Thom SA, Hughes AD. Wave-energy patterns in carotid, brachial, and radial arteries: a noninvasive approach using wave-intensity analysis. *Am J Physiol Heart Circ Physiol* 2005;**289**(1):H270—6.
11. Baruch MC, Warburton DE, Bredin SS, Cote A, Gerdt DW, Adkins CM. Pulse decomposition analysis of the digital arterial pulse during hemorrhage simulation. *Nonlinear Biomed Phys* 2011;**5**(1):1.
12. Westerhof BE, Guelen I, Westerhof N, Karemaker JM, Avolio A. Quantification of wave reflection in the human aorta from pressure alone: a proof of principle. *Hypertension* 2006;**48**(4):595—601.
13. Goswami D, Chaudhuri K, Mukherjee J. A new two-pulse synthesis model for digital volume pulse signal analysis. *Cardiovasc Eng* 2010;**10**(3):109—17.
14. Rubins U. Finger and ear photoplethysmogram waveform analysis by fitting with Gaussians. *Med Biol Eng Comput* 2008;**46**(12):1271—6.
15. Huotari M, Vehkaoja A, Määttä K, Kostamovaara J. Pulse waveforms are an indicator of the condition of vascular system. *Ifmbe Proc* 2013;**39**:526—9.
16. Huotari M, Vehkaoja A, Määttä K, Kostamovaara J. Photoplethysmography and its detailed pulse waveform analysis for arterial stiffness. *J Mech Mater Struct* 2011;**44**(4):345—62.
17. Wang L, Xu L, Feng S, Meng QH, Wang K. Multi-Gaussian fitting for pulse waveform using weighted least squares and multi-criteria decision making method. *Comput Biol Med* 2013;**43**(11):1661—72.
18. Couceiro R, Carvalho P, Paiva RP, Henriques J, Quintal I, Antunes M, et al. Assessment of cardiovascular function from multi-Gaussian fitting of a finger photoplethysmogram. *Physiol Meas* 2015;**36**(9):1801—25.
19. Liu C, Zheng D, Murray A, Liu C. Modeling carotid and radial artery pulse pressure waveforms by curve fitting with Gaussian functions. *Biomed Signal Process Contr* 2013;**8**(5):449—54.
20. Mao CG, Guo XQ, Zhou H, Xie YZ. Fitting method of the simulated HEMP waveform by the double-exponential function. *High Power Laser Part Beams* 2004;**16**(3):336—40.
21. Jiang X, Wei S, Zheng D, Liu F, Zhang S, Zhang Z, et al. Change of bilateral difference in radial artery pulse morphology with one-side arm movement. *Artery Res* 2017;**19**:1—8.
22. Zong W, Heldt T, Moody GB, Mark RG. An open-source algorithm to detect onset of arterial blood pressure pulses. *Comput Cardiol* 2013;**25**:259—62.
23. Liu C, Li Q, Clifford GD. *Evaluation of the accuracy and noise response of an open-source pulse onset detection algorithm on pulsatile waveform databases[C]//Computing in Cardiology Conference*. IEEE; 2017.
24. Liu C, Zhuang T, Zhao L, Chang F, Liu C, Wei S, et al. Modelling arterial pressure waveforms using Gaussian functions and two-stage particle swarm optimizer. *BioMed Res Int* 2014;**2014**:923260.
25. He D, Wang L, Fan X, Yao Y, Geng N, Sun Y, et al. A new mathematical model of wrist pulse waveforms characterizes patients with cardiovascular disease — a pilot study. *Med Eng Phys* 2017;**48**:142—9.
26. Allen J. Photoplethysmography and its application in clinical physiological measurement. *Physiol Meas* 2007;**28**(3):R1—39.